ISBN: 978-3-95450-262-2 ISSN: 2673-5350 doi: 10.18429/JACoW-IBIC2025-MOPCO33

STATUS OF THE SOURCE OF POLARIZED ELECTRONS AT ELSA WITH IMPROVED LASER AND ELECTRON BEAM DIAGNOSTICS

M. Switka*, K. Desch, D. Proft, A. Spreitzer, Physics Institute, University of Bonn, Bonn, Germany

Abstract

The ELSA facility at the University of Bonn uses a storage ring to accelerate polarized electrons up to 3.2 GeV. The photoinjector source is driven by a Ti:Sa laser beam to obtain a high polarization degree (~86 %) from a GaAsP strained-layer superlattice crystal photocathode. After a prolonged shutdown of the source we restored its status to *fully operational* and fine-tuned the laser system, the crystal storage and cleaning apparatus as well as the Linac transfer beamline. The in-house developed diagnostic software FGrabbit has been employed for the analysis of laser and electron beam camera images, providing increased precision and dynamic range in the optimization process. The impact of the crystal cleaning process was studied with spatially resolved quantum efficiency mapping of the photocathode surface.

INTRODUCTION

The source of polarized electrons at the ELSA facility [1] had not been in use since 2017 due to minor defects in the subsystems and subordinate demand from the experimental program. However, upcoming experiments [2] favor photoproduction with polarized electrons, having lead to a reactivation effort of the required source. After repairs of water cooling and electrical infrastructure the source initially showed poor performance, demanding extensive analysis and fine-adjustment of all involved subsystems: The Ti:Sa laser pulse energy had to be increased from 2 mJ to 20 mJ by optimizing resonator and subsequent laser beamline, the quantum efficiencies of the available photocathodes had to be increased by an order of magnitude as well as the electron transfer beamline efficiency to the Linac.

DESIGN OF THE POLARIZED ELECTRON SOURCE

The 50 kV source of polarized electrons at ELSA has been developed by W. Hillert [3] and extended by D. Heiliger [4] with crystal storage and hydrogen cleaning chambers (see Fig. 1). Up to six crystals can be stored and activated by heat- and atomic hydrogen cleaning procedures with subsequent deposition of caesium oxide on the crystal surface, to restore their quantum efficiency. A 4 mJ laser pulse (at 780 nm for GaAs/GaAsP crystals) is required to generate a 200 mA electron pulse for 1 µs duration, which is transferred to the 26 MeV Linac.

Titanium Sapphire Laser and Photon Beamline

A free running 50 Hz flashlamp-pumped Ti:Sa laser generates laser pulses of up to 200 mJ and 10 µs length. To

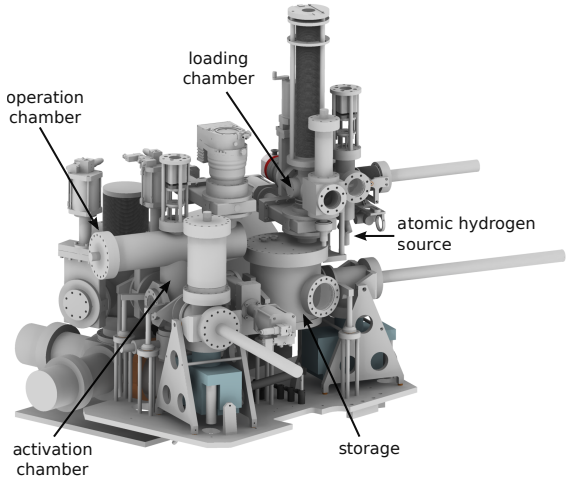

Figure 1: Overview of the source assembly with operation chamber, crystal activation-, storage- and loading chambers [4]. The latter includes a source for atomic hydrogen cleaning.

synchronize the useful part of the laser pulse precicely with the Linac RF timing, a pulse picker setup is used consisting of a triggered Pockels cell and polarizing beam splitter (see Fig. 2). It transmits 20 mJ towards a ~ 80 m long optical fiber, transporting the laser beam to the source assembly [5]. The multimode fiber defines the beam profile and leads to full polarization loss, requiring repolarization with a combined polarizing beam splitter and switchable $\lambda/4$ Pockels cell. The transfer efficiency of approximately 20 % provides 4 mJ circularly polarized laser pulses with alternating helicity, fully illuminating the GaAs-based photocathode crystals in the operation chamber.

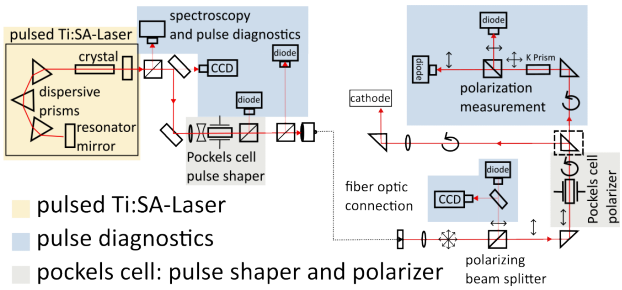

Figure 2: Sketch of the Ti:Sa laser photon beamline with pulse shaper and polarizer [5] with improved diagnostics.

Photocathode

The GaAs/GaAsP strained-layer superlattice crystal photocathode [6] diameter amounts 8.9 mm and is illuminated

* switka@physik.uni-bonn.de

ISBN: 978-3-95450-262-2 ISSN: 2673-5350 doi: 10.18429/JACoW-IBIC2025-MOPCO33

by a Gaussian photon intensity profile. Its design goal is to provide 200 mA of current within the space-charge limit, to be transferred into the Linac.

Linac Transfer Beamline

The approximately 7 m long electron transfer beamline includes a symmetric U-shaped section, followed by an electrostatic deflector guiding the beam sideways while preserving the spin direction in the vertical plane. This aligns it with the magnetic field of the bending magnets of the subsequent synchrotrons. Beamline calculations show that quasi lossless transport is feasible with this setup [1].

SOURCE PERFORMANCE STATUS

Laser Pulse

In first reactivation attempts, the 50 Hz flashlamp-pumped Ti:Sa laser initially lacked a factor of ten in pulse energy. The main optimization efforts were concentrated on fine-tuning the resonator setup. Analysis of the resonator modes via the outcoupled laser beam (see Fig. 2) allowed for systematic tuning and optimum mode selection. As the pulse shape dissolves during the fiber transport (see Fig. 3) maximum pulse energy was achieved by occupying the fibre with a multitude of transverse laser modes. The expected pulse energy of up to 200 mJ and the spectral response of the Ti:Sa laser could be fully restored.

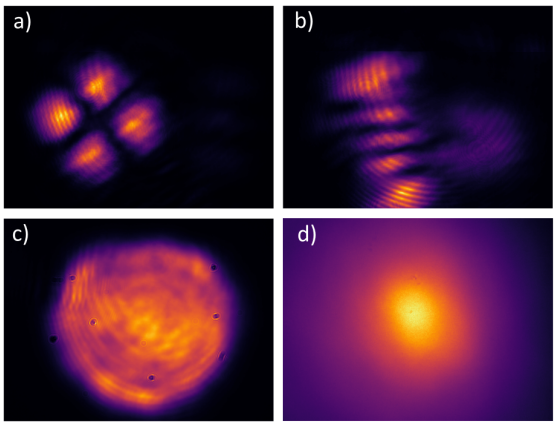

Figure 3: a) and b) show different laser modes in the resonator, c) shows a multitude of transverse laser modes, which dissolve during the transport in the optical fiber d).

To meet the temporal acceptance of the Linac RF a 1 µs 20 mJ pulse is picked out of the full structure by a pulse picker setup (see Fig. 2). In Fig. 4 the temporal structure of both the transmitted and dumped laser pulse is shown. The chosen selection of the typical Ti:Sa excitation structure provide a sufficient compromise in overall pulse energy an homogeneity to reach the targeted 20 mJ pulse before injection into the fibre.

Photocathodes

The GaAs/GaAsP strained-layer superlattice crystals currently in use provide quantum efficiencies of up to 2.02 %

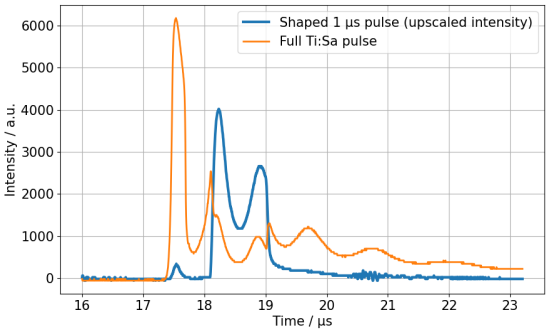

Figure 4: Blue: Picked 1 µs pulse with 20 mJ pulse energy. Orange: Dumped primary Ti:Sa pulse with visible cut-out.

at $\lambda = 633$ nm (0.06 % at 780 nm). Polarization degrees of 86 % are typical and 82.6(6) % have been measured recently via Mott scattering. Both, heat an atomic hydrogen cleaning stations are operational and allow frequent restoration of the naturally decreasing quantum efficiencies.

Beamline Optimization

With achieved design laser pulse energy and crystal quantum efficiencies, the electron transfer beamline could be optimized. Visual feedback from laser and electron screens in combination with the large dynamic range of modern digital cameras (~ six orders of magnitude) and application of the in-house developed camera readout-out system FGrabbit [7] showed to be very useful for initial beam guiding. Electron signals could be maximized by iterative optimization of more than 32 guiding and focusing devices.

We successfully ran the facility in standard operation with the photoinjector source. It delivers electron beam currents similar to the regularly used thermionic electron source, including sufficient overhead for an expected decrease in photocathode efficiency during regular operation.

CRYSTAL ACTIVATION AND CLEANING PERFORMANCE

To obtain high levels of quantum efficiency (QE) for GaAs-type crystals, a mono-atomic layer of caesium-oxide is deposited on the crystal surface to achieve negative electron affinity (NEA). Oxidation from interaction with residual gas leads to a degradation of the quantum efficiency with time, expressed by the lifetime τ for which the QE after activation has decreased to $1/e$. Therefore a heat cleaning and atomic hydrogen cleaning procedure [4] and alternating deposition of caesium and oxygen afterwards is applied, as shown in Fig. 5. Two GaAs/GaAsP strained-layer superlattice crystals were investigated in detail. Crystal #1, which had last been used successfully in 2017, showed a QE of 1.2 % after its first reactivation in 2023. However, subsequent heat-cleaning and activation cycles resulted in progressively lower QEs, reaching only up to 0.13 %, indicating that significant impurities had built up and could only be removed by atomic hydrogen cleaning. In contrast, crystal #2 showed adequate

ISBN: 978-3-95450-262-2 ISSN: 2673-5350 doi: 10.18429/JACoW-IBIC2025-MOPCO33

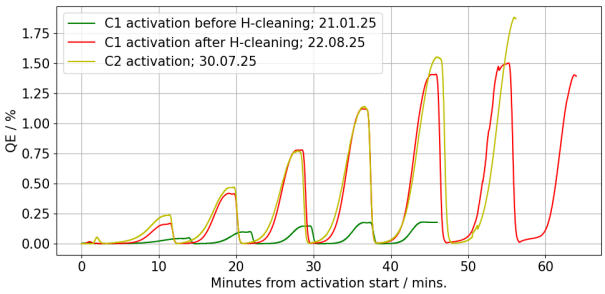

Figure 5: Activation cycles of crystal #1, before vs. after atomic hydrogen cleaning and activation of crystal #2

activation behavior with yet increasing achievable QE for each heat cleaning procedure, reaching up to 2.02 %. Lifetimes of typically $\tau = 280(60)$ h are observed, providing sufficient charge for long-term operation.

QE Mapping and Atomic Hydrogen Cleaning

To gain deeper insight into the surface properties of the activated crystals, a two-dimensional QE mapping procedure (compare with [8]) was implemented, as shown in Fig. 6. A 633 nm laser beam with a spot size of 25 µm is scanned linearly across the crystal surface inside the activation chamber. The QE is determined from a simultaneous measurement of laser power and emission current, where the resolution is defined by the step spacing of the used linear translation stages. It is noticeable that the QE scan reveals a crescent-like structure observed on crystal #1. Application of the

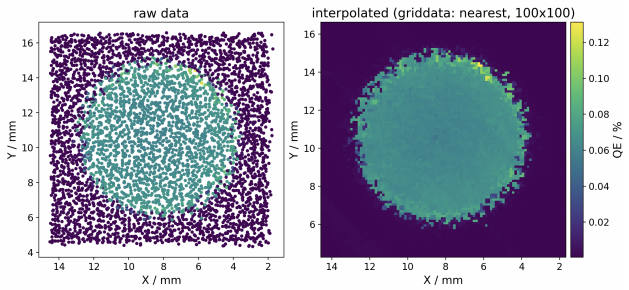

Figure 6: 2D QE scan of crystal #2 25 days after activation. Left: scatter plot of raw data, right: interpolated data.

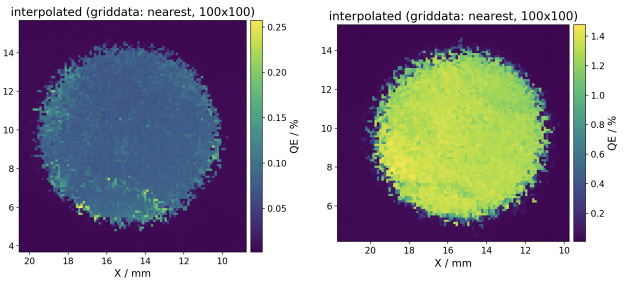

Figure 7: QE scan of crystal # 1 before (left) and after atomic hydrogen cleaning (right).

atomic hydrogen cleaning procedure (with simultaneous heat cleaning at 450 °C) lead to a significant recovery of its obtainable QE towards the 1 % level. The QE map of crystal #1 after hydrogen cleaning is shown in Fig. 7, where the characteristic substructure is still observable. It could also not be removed by follow-up heat and atomic hydrogen cleaning procedures (both at 550 °C), suggesting a minor structural deficit or surface contamination, which cannot be removed with the available cleaning methods. However, an increase of its overall QE to 1.56 % could be achieved.

CONCLUSION

The source of polarized electrons at ELSA has been successfully recommissioned and optimized after several years of inactivity. Visual diagnostic improvements enabled systematic optimization of both laser and electron beams. A 2D spatial QE scan was implemented to diagnose the crystal quality and to monitor the impact of the cleaning procedures in greater detail. The source now reliably provides polarized electrons suitable for upcoming experiments and long-term operation.

REFERENCES

[1] W. Hillert *et al.*, "Beam and spin dynamics in the fast ramping storage ring ELSA", *EPJ Web Conf.*, vol. 134, p. 05002, Jan. 2017. doi:10.1051/epjconf/201713405002

[2] Color Meets Flavor, `https://www.color-meets-flavor.de/`

[3] W. Hillert, "The Bonn Electron Stretcher Accelerator ELSA: Past and future", *Eur. Phys. J. A*, vol. 28, pp. 139–148, 2006. doi:10.1140/epja/i2006-09-015-4

[4] D. Heiliger, W. Hillert, and B. Neff, "A new load lock system for the source of polarised electrons at ELSA", in *Proc. IPAC'13*, Shanghai, China, May 2013, paper MOPFI006, pp. 294–296.

[5] M. Gowin, "Optimierung der laserinduzierten Photoemission zur Erzeugung polarisierter Elektronenstrahlen an der 50 keV-Quelle der Bonner Beschleunigeranlage ELSA", Ph.D. thesis, Phys. Dept., University of Bonn, Bonn, Germany, 2001.

[6] F. Furuta *et al.*, "Highly polarized electrons from GaAs-GaAsP and InGaAs-AlGaAs strained layer superlattice photocathodes", in *Proc. LINAC'04*, Lübeck, Germany, Aug. 2004, paper THP24, pp. 648–650.

[7] M. Switka *et al.*, "Progress on distributed image analysis from digital cameras at ELSA using the RabbitMQ message broker", in *Proc. IBIC'23*, Saskatoon, Canada, Sep. 2023, pp. 449–452. doi:10.18429/JACoW-IBIC2023-WEP046

[8] M. Herbert *et al.*, "Enhanced durability NEA surface layer for GaAs photocathodes using Cs, O_2, and Li", in *Proc. PSTP2024*, Jefferson Lab, Newport News, VA, USA, Sep. 2024, p. 055. doi:10.22323/1.472.0055